Multi-AUV Marine Life Tracking via Single Transceiver Payloads

Christopher Herrera, Caitlyn Ossa, Yoo-Jin Hwang, Declan O'Neill, Alberto Soto, Christopher Clark
Harvey Mudd College
Claremont, United States
ciherrera,cossa,yhwang,doneill,alsoto,clark@g.hmc.edu

Christopher G. Lowe
California State University Long Beach
Long Beach, United States
chris.lowe@csulb.edu

ABSTRACT

This paper presents and validates a multi-autonomous underwater vehicle (AUV) tracking system for localizing acoustic tags that typically are affixed to fish. This work is motivated by the current limitations in the tracking of marine animals. The work presented is a key component for a multi-AUV system that can autonomously follow tagged marine animals with increased temporal and spatial resolution and accuracy. A single compact omnidirectional acoustic receiver, called the Rx-Live receiver, is mounted on each AUV which reduces drag compared to multi-hydrophone payloads. To fuse the acoustic measurements received by multiple AUVs, a particle filter algorithm is used which outputs the estimated state (e.g. position) of the acoustic tag. To validate the system, multiple receivers and tags were deployed in ocean environments that are habitats for several species of interest, e.g., nurse sharks and white sharks. The algorithm was tested on multiple datasets including one in which the tag and receivers are stationary, and one in which the tag and receivers all moved dynamically. The estimated trajectories of the acoustic tag produced by the algorithm were compared to groundtruth GPS trajectories of the tag and achieved a root mean square error (RMSE) of approximately 10 meters after convergence.

KEYWORDS

underwater robotics, multi-robot system, state estimation

ACM Reference Format:
Christopher Herrera, Caitlyn Ossa, Yoo-Jin Hwang, Declan O'Neill, Alberto Soto, Christopher Clark and Christopher G. Lowe. 2023. Multi-AUV Marine Life Tracking via Single Transceiver Payloads. In *Proc. of the 22nd International Conference on Autonomous Agents and Multiagent Systems (AAMAS 2023), London, United Kingdom, May 29 – June 2, 2023*, IFAAMAS, 7 pages.

1 INTRODUCTION

In recent years, a multitude of studies have been conducted on the movements and migratory patterns of marine animals, the data for which have been gathered using acoustic telemetry-based tracking. Tagged animals can be tracked passively by static receivers, or actively by researchers follow the animal using a surface-based directional receiver system. Both approaches present unique challenges: passive tracking has a fixed detection area outside of which no data is collected, while active tracking requires hours of manual labor resulting in limited run times. Autonomous tracking using AUVs with mounted hydrophones addresses many of the challenges with both approaches. It allows the receivers to move with the animal and greatly reduces the manual labor and onsite requirements of the researchers. However, it also brings its own challenges including limitations on AUV battery life, the need to minimize AUV-marine life interactions, AUV obstacle avoidance, and a general increased level of complexity. Additionally, past approaches have utilized AUVs equipped with a large payload holding two hydrophones at each end, separated by the length of the AUV. The payload makes state estimation easier but induces a considerable amount of drag

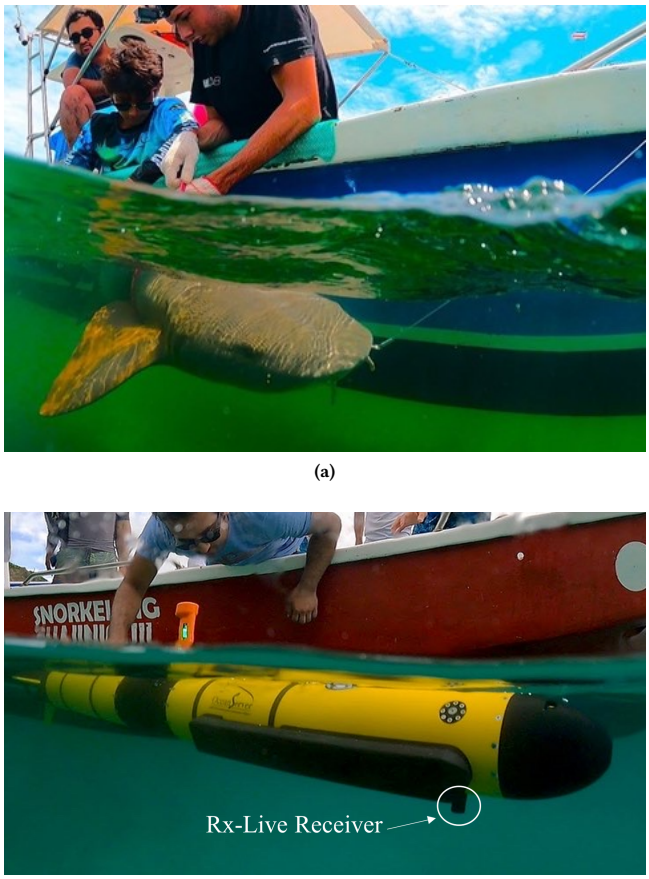

(a)

(b)

Figure 1: Marine life tracking with AUVs. (a) A nurse shark being fitted with an acoustic transmitter for tracking its movements. (b) AUV with Rx-Live Receiver during a field deployment.

Proc. of the 22nd International Conference on Autonomous Agents and Multiagent Systems (AAMAS 2023), A. Ricci, W. Yeoh, N. Agmon, B. An (eds.), May 29 – June 2, 2023, London, United Kingdom.

leading to reduced battery life and maneuverability [10, 11]. One solution which has been implemented in the past is to enable two way communication between the tag and AUV. This allows for position estimation without the large hydrophone payload but at the cost of requiring a larger and more complex custom tag to be attached to the animal, limiting the size of animals that can be tracked [7, 9].

In developing a strategy that enables multiple AUVs, each equipped with a single receiver, to track marine life affixed with acoustic transmitters, the following contributions have been made:

(1) An approach to measuring distance using a single omnidirectional acoustic receiver and an off-the-shelf tag, of which 10,000 plus are currently deployed in our oceans.
(2) A multi-robot particle filter for estimating the location of an acoustic tag with said receivers.
(3) Offline validation of the particle filter with experimental data from real ocean deployments.

This paper is organized as follows: Section 2 provides relevant background regarding previous work with hydrophones, AUVs, filters, and marine-life tracking methods. Section 3 provides a system overview and describes the multi-robot particle filter. Section 4 describes the field experiments performed to collect data. Section 5 presents and analyzes the results of running the particle filter offline on that data. Finally, Section 6 explains the impact of this paper and describes future work.

2 BACKGROUND

In the past, researchers have used satellite tags, acoustic telemetry, stationary reciever arrays, and manually controlled boats to track the motion patterns of individual fish [3, 4, 8, 12–17]. However, each of these methods require certain conditions for accuracy such as ensuring that the fish remains near the surface of the water. When determining the position of an animal, a manually controlled boat can be used but it requires continuous repositioning of the boat with respect to the movements of the fish below and the tracking quality is conditional on the human's ability [3, 8, 12, 14, 17]. As such, in recent years, scientists have developed AUV tracking systems to mitigate the inconsistencies and requirements previously needed to track marine life [1, 2, 6]. For example, AUVs have been equipped with GPS, 3-axis compass, state estimation processors, and a stereo-hydrophone receiver system that listens for acoustic transmitters attached to the marine life being tracked [17]. The receiver system provides "differential time of arrival data necessary for state estimation," which is then processed using the particle filter [5]. These robots were found to have "significantly better spatial accuracy" than human-based active tracking as well as a "higher frequency of accurate location estimates," with positional errors being less than ten meters [18]. In 2012, a team of researchers added a particle filter to their AUV in an effort to enable real-time state estimation of sharks and other marine life, including their position, orientation, velocity, and weight, in the immediate area [5]. With multiple AUVs running during testing, this dramatically increased the accuracy when determining an animal's location and movements. However, due to the additional weight and drag of the multi-hydrophone payloads, the AUVs were considerably slower and harder to maneuver than without the hydrophones.

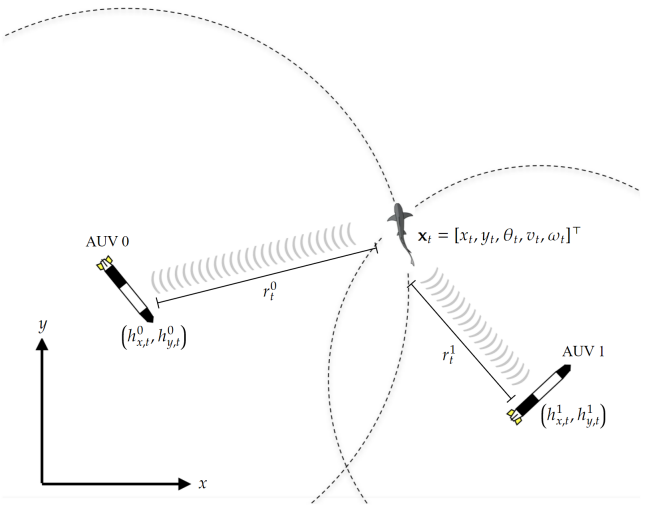

Figure 2: Top down view of two Rx receiver equipped AUVs estimating the geoposition of an acoustically tagged shark.

To improve the efficiency of the AUVs, the new system replaces the multi-hydrophone payload with a single omnidirectional hydrophone placed within each robot, as shown in Figure 1b. The new setup's compact nature allows the AUV to move at greater speeds for an increase in mobility and maneuvering. With multiple AUVs in the water and this system in place, larger data sets can be collected in a shorter period of time, thus increasing the efficiency and quantity all the while ensuring the quality of the data.

Together, these contributions form a key component for a new system of sensing and an enhanced method of state estimation for highly mobile tagged marine-life animals. This tracking system was validated through real ocean deployments to test the hardware and software which will be discussed throughout the paper.

3 MULTI-ROBOT SYSTEM

3.1 System Overview

The multi-robot system consists of two AUVs and an acoustic tag as shown in Figure 2. The acoustic tag emits signals which the AUVs are capable of detecting via mounted omnidirectional hydrophones. While the system is 3 dimensional, for the current work it is assumed that the AUVs and the tag remain close to the surface at all times, allowing the use of 2D positions and orientations. This assumption is valid since during field experiments, the tag and hydrophones were deployed in shallow water and remained near the surface. For the general case where full 3D state estimation is needed, acoustic tags that include depth sensors have successfully been used for 3D position state estimation in other AUV tracking work [10]. In this system, the AUV states (i.e. positions, orientations, and velocities) are known via on board sensing (e.g. GPS, compass, DVL), but the tag's state is unknown. The state $\mathbf{x}$ to be estimated consists of the tag's x and y coordinates, its orientation θ, its linear speed v, and its angular velocity ω

$$\mathbf{x}_t = [x_t^i, y_t^i, \theta_t^i, v_t^i, \omega_t^i]^\top. \tag{1}$$

3.2 Distance Estimation

The first step to estimating the state of the tag is estimating the distances between it and each AUV. The tag emits signals at a constant rate of approximately 0.125 Hz, or once every 8 seconds, with the exact value depending on the specific tag. The hydrophone mounted on the AUV actively listens for these signals and has some probability of detecting them depending on the distance, the amount of ambient noise, and whether they have a clear line of sight to the tag. When a detection occurs, the hydrophone receiver outputs the tag's ID, an estimate of the signal's strength, and the time t at which the detection occurred. If the signal's time of flight (TOF) τ_t were known, then the distance r_t between the hydrophone and tag could be computed by multiplying τ_t by the speed of sound in water ($s = 1460$ m/s). Unfortunately τ_t cannot be measured directly, but the amount by which the TOF has changed between detections, $\Delta\tau_t$, can be used to estimate it. By comparing the difference in time Δt between subsequent detections with the tag's known period T between signals, it is possible to compute $\Delta\tau_t$. If Δt is greater than T, this indicates that the tag has moved further from the hydrophone in the time between the two detections, and vice versa. To start, the change in TOF can be calculated as a function of the period T and the measurement δt:

$$\Delta\tau_t = \text{mod}\left(\Delta t - \frac{1}{2}T, T\right) - \frac{1}{2}T. \tag{2}$$

In equation (2) above it is necessary to use modular arithmetic instead of just subtracting T because it is possible for the hydrophone to miss one or more signals, in which case the time between detections given no change in r_t would be a multiple of T. Changes in distance between detections Δr_t can then be computed as:

$$\Delta r_t = r_t - r_{t-1} = s\Delta\tau_t, \tag{3}$$

$$\Delta r_{0:t} = r_t - r_0 = \Delta r_t + \cdots + \Delta r_1. \tag{4}$$

Starting the system with the tag next to the hydrophone guarantees that $r_0 = 0$, which means $\Delta r_{0:t} = r_t$. The relative speed between the hydrophone and tag can also be approximated as $\dot{r}_t = \frac{\Delta r_t}{\Delta t}$.

Figure 3 compares the groundtruth distance between the tag and the hydrophone measured using GPS coordinates with distances computed using the TOF method described. In Figure 3, the label 'TOF distance' refers to $\Delta r_{0:t}$ where $r_0 \neq 0$ and as seen in the top panel, this results in an offset from the true distance. The label 'Shifted TOF distance' refers to $\Delta r_t = r_{0:t} + r_0$ computed using the initial GPS distance as r_0. Unfortunately, the clocks used by the AUV computers, the tags, and the hydrophones are all subject to drift. Although it starts close to the groundtruth distance, Figure 3's bottom panel shows that as time passes the drift in r_t increases, i.e. the error grows. The 'Adjusted TOF distance' attempts to correct for this drift by linearly interpolating between the errors at the initial and final times to approximate the error in r_t for any time t. This approximated error is subtracted from the TOF distance resulting in the most accurate measurement of distance. Note that this approach requires knowing both the initial and final groundtruth distances, which can be accomplished if the system both starts and ends with the tag next to the hydrophone. The subsequent results presented use the shifted TOF r_t as a compromise between accuracy and required knowledge of true distances.

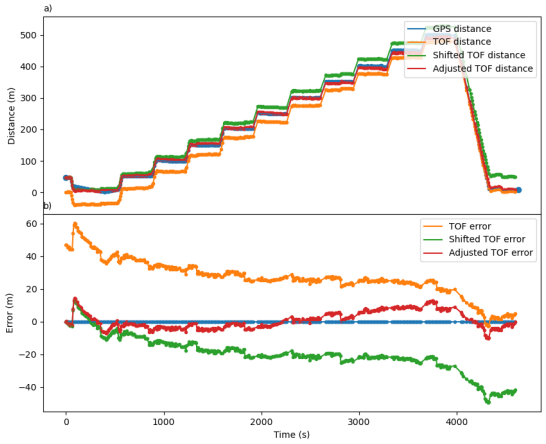

Figure 3: TOF distance estimates. (Top panel) TOF distance estimates and groundtruth GPS distance. (Bottom panel) Error in meters for each TOF distance estimate.

3.3 Particle Filter

The particle filter is a state estimation algorithm that uses a collection of particles to represent a probability distribution over the state. It consists of a prediction and correction step. While no new measurements are available, the prediction step propagates particles forward in time according to a motion model. As measurements are received, the correction step assigns weights to each particle using a measurement model and resamples the particles. Resampling consists of drawing a new set of particles from the old set with probabilities proportional to the weights and with replacement.

Particle i at time t and the set of particles at time t are denoted respectively as

$$p_t^i = [x_t^i, y_t^i, \theta_t^i, v_t^i, \omega_t^i, w_t^i]^\top, \tag{5}$$

$$P_t = \{p_t^1, \ldots, p_t^n\}. \tag{6}$$

where w is the particle's weight and n is the number of particles. A measurement z_t at time t consists of the distance r between a hydrophone and the tag, and its time derivative $\dot{r}$

$$z_t = [r_t, \dot{r}_t]^\top. \tag{7}$$

These are obtained for each detection using the TOF method described previously. Algorithm 1 provides pseudocode for initializing the particle filter.

Algorithm 1 Particle Filter Initialization(n)

// Initialize particles uniformly randomly
for $i = 1$ to n **do**
    sample $x_0^i, y_0^i \sim U(x_{\min}, x_{\max}), U(y_{\min}, y_{\max})$
    sample $\theta_0^i \sim U(-\frac{\pi}{2}, \frac{\pi}{2})$
    $p_0^i = [x_0^i, y_0^i, \theta_0^i, 0, 0, 1]^\top$
end for
$P_0 = \{p_0^1, \ldots, p_0^n\}$

3.3.1 Prediction Step. On each prediction step, random numbers Δx and Δy are sampled from Gaussians with mean 0 and are added to each particle's current x_t and y_t coordinates to produce x_{t+1} and y_{t+1}. The particles' new angles and new velocities are calculated using the old and new coordinates, and the new particles' weights are set to the old particles' weights. The ith particle at time $t+1$ is given by

$$p_{t+1}^i = \begin{bmatrix} x_t + \Delta x \\ y_t + \Delta y \\ \text{atan2}(\Delta y, \Delta x) \\ \frac{\sqrt{\Delta x^2 + \Delta y^2}}{\Delta t} \\ \frac{\theta_{t+1} - \theta_t}{\Delta t} \\ w_t \end{bmatrix} \tag{8}$$

Prediction steps are scheduled at regular 1 second intervals.

3.3.2 Correction Step. Let $Z_t = \{z_t^0, \ldots, z_t^m\}$ be the set of m measurements available during the correction step. If both hydrophones detected the same signal from the tag, two measurements will be available nearly simultaneously. Otherwise, only one or zero measurements could be available. If Z_t is not empty, then the particles are weighted by comparing the true measurements z_t^j with the predicted measurements $\hat{z}_t^{i,j}$ given the ith particle's state. The predicted distance and relative speed for particle i and measurement j are given by

$$\hat{r}_t^{i,j} = \sqrt{(h_{x,t}^j - x_t^i)^2 + (h_{y,t}^j - y_t^i)^2}, \tag{9}$$

$$\hat{\dot{r}}_t^{i,j} = \frac{(h_{x,t}^j - x_t^i)(\dot{h}_{x,t}^j - \dot{x}_t^i) + (h_{y,t}^j - y_t^i)(\dot{h}_{y,t}^j - \dot{y}_t^i)}{\hat{r}_t^{i,j}}. \tag{10}$$

where $h_{x,t}^j$, $h_{y,t}^j$, $\dot{h}_{x,t}^j$, and $\dot{h}_{y,t}^j$ are the x and y coordinates and x and y velocities respectively of the hydrophone that produced measurement j at time t. The predicted measurements are then used to update the weights as follows

$$w_t^i = \Pi_{j=1}^m \mathcal{N}(\hat{z}_t^{i,j} | z_t^j, \Sigma), \tag{11}$$

where Σ is the measurement covariance matrix whole value is given as a parameter of the particle filter. The final weight is the joint probability of all of the measurements, assuming independence. All weights are set to 1 the first time the particles are created and after every resample.

Resampling occurs after all measurements between prediction steps have been processed. It is advantageous not to resample between simultaneous measurements in order to maintain particle diversity. This also ensures that resampled particles do not depend on the order that the measurements were processed. Algorithm 2 provides pseudocode for one iteration of the algorithm which performs a prediction step and a correction step if necessary for every time step t. Its inputs are the particles P_t and measurements Z_t.

Algorithm 2 Particle Filter Iteration(P_t, Z_t)

```
// Prediction step
for p_t^i in P_t do
    sample p_{t+1}^i ~ Pr(x_t | p_t^i) // Implemented by equation (8)
end for
P_{t+1} = {p_{t+1}^1, ..., p_{t+1}^n}

// Correction step
if Z_t ≠ ∅ then
    for p_t^i in P_t do
        w_t^i = Π_{z_t ∈ Z_t} Pr(z_t | p_t^i)
    end for

    // Resample
    P_{t+1} = ∅
    for i = 1 to n do
        draw i from {1, ..., n} with probability ∝ w_t^i
        add a copy of p_t^i to P_{t+1} with weight set to 1
    end for
end if
```

4 FIELD DEPLOYMENTS

To collect data to validate the distance estimation and particle filter, the hydrophones and acoustic tag were deployed multiple times off the coast in Long Beach, CA and in Santa Elena Bay, Costa Rica. The data shown in Figure 3 is from a Long Beach deployment in which the tag was anchored with a buoy at known coordinates. An AUV with a mounted Rx-Live receiver then followed predetermined paths, driving farther and farther from the tag before returning. The AUV's built-in GPS and state estimation software was used to obtain groundtruth distances. A boat containing a laptop PC connected to another Rx-Live receiver and a USB GPS was anchored near the tag throughout this test and also recorded detections and coordinates.

Two additional datasets collected in Costa Rica were used to validate the particle filter. In both datasets, two hydrophones recorded detections and coordinates from a tag deployed in Santa Elena Bay. The first dataset, called the static dataset, was collected on July 19, 2022. Two boats containing hydrophones and a tag were anchored in place throughout the deployment. Tag detections and coordinates of the boats were then recorded for 760 seconds, or 12 minutes and 40 seconds. Unlike the boats which recorded their coordinates continuously, the tag's coordinates were only recorded once when the buoy it was anchored to was deployed. The two boats and tag were roughly co-linear along the surface of the water, with the tag placed in between the two boats.

The second dataset, called the dynamic dataset, was collected on July 21, 2022. Both hydrophones as well as the tag moved throughout this deployment which lasted about an hour. Neither the boats nor the tag were anchored in place. The boats were allowed to drift for most of the deployment but were moved when necessary to stay near the tag. The tag was moved near the shore of Santa Elena bay by a swimmer. As with the static dataset, the boats continuously recorded tag detections and coordinates. The tag's coordinates were recorded continuously by a waterproof GPS watch carried along by the swimmer. There were substantial gaps in the watch's coordinates resulting in long periods without groundtruth. The dynamic dataset consists of 349 seconds, or 5 minutes and 49 seconds during which the watch's coordinates were recorded and there were a substantial number of detections by both hydrophones.

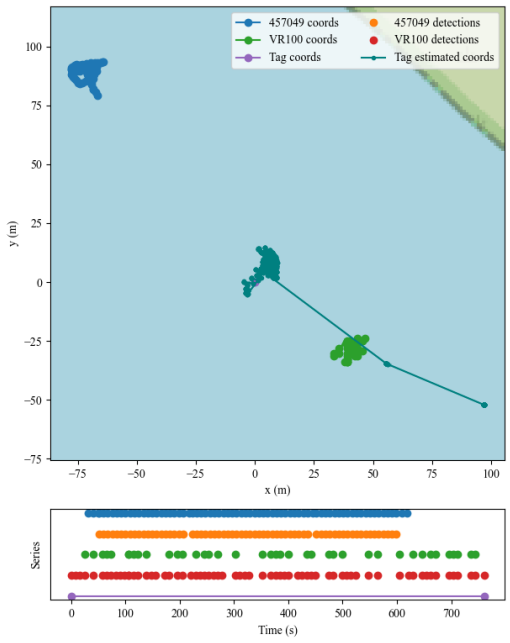

Figure 4: Static deployment data. (Top panel) The trajectories of the hydrophones and the tag. (Bottom panel) Timing of GPS coordinate acquisition and tag detection events.

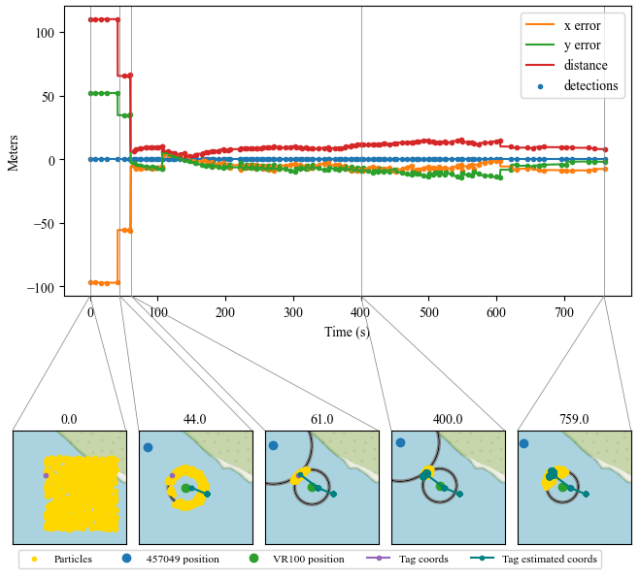

Figure 5: Static dataset prediction errors. (Top panel) Estimated tag x, y, and position errors. (Bottom 5 panels) Particle distribution at different points in time.

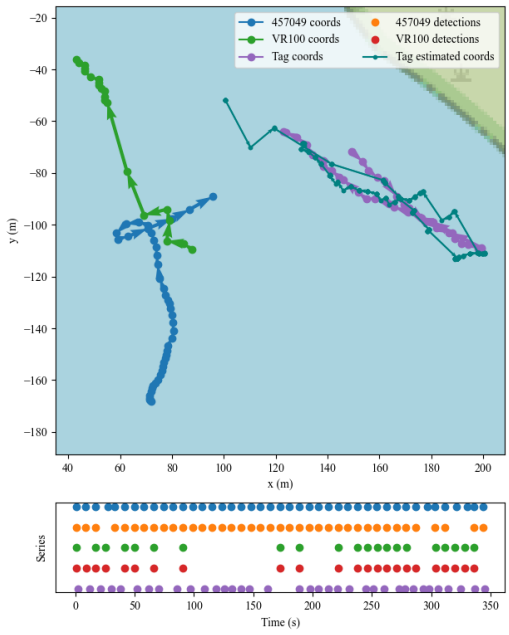

Figure 6: Dynamic deployment data. (Top panel) The trajectories of the hydrophones and the tag. (Bottom panel) Timing of GPS coordinate acquisitions and tag detection events.

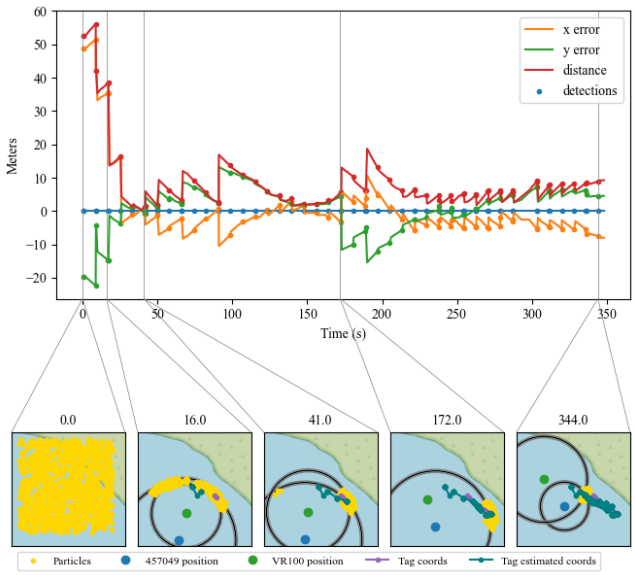

Figure 7: Dynamic dataset prediction errors. (Top panel) Estimated tag x, y, and position errors. (Bottom 5 panels) Particle distribution at different points in time.

5 VALIDATION

5.1 Static Dataset

The top panel in Figure 4 shows the trajectories of the two hydrophones and the tag in the static dataset, as well as the estimated

Table 1: Static Dataset Errors

Time span	Distance (m)			RMSE (m)
	Max	Average	Stdev	
0s to end	110.19	16.27	23.69	28.74
61s to end	15.16	9.72	2.82	10.12

Table 2: Dynamic Dataset Errors

Time span	Distance (m)			RMSE (m)
	Max	Average	Stdev	
0s to end	56.14	8.60	10.16	13.31
30s to end	18.69	6.10	3.52	7.04

trajectory of the tag produced by the particle filter. All trajectories are plotted over a map of Santa Elena Bay. The bottom panel in Figure 4 shows the times at which each hydrophone's GPS coordinates were recorded as well as the times at which each hydrophone detected the tag. The dataset contains 66 detections from hydrophone 457049 and 66 detections from hydrophone VR100 spanning 760 seconds. Since the tag was deployed on a stationary buoy, its GPS coordinates were recorded only at the time of deployment. While hydrophone VR100 received detections the entire time, hydrophone 457049 started receiving detections slightly later and stopped receiving them 2 minutes before the other hydrophone.

Figure 5 compares the estimated tag position to the true tag position at each point in time. The differences in x and y coordinates as well as the distance between the estimate and true positions are plotted. Points in time at which a detection from either hydrophone was received are plotted as dots. The lower panels in Figure 5 show the state of the particle filter at different points in time. Particles are plotted as dots and the circles show the estimated distances from each hydrophone to the tag, as well as one standard deviation around the estimate. At the start, the particles are initialized randomly since the tag's initial position can not be assumed to be known, as seen in the panel at 0 seconds. While only hydrophone VR100 has detected the tag, the particles cluster in a circle around its location as seen in the second panel at 44 seconds. After 61 seconds, both hydrophones have received detections so the particles converge at the intersection of both ranges as seen in the third lower panel. The particles continue to gather tightly around the tag's location until hydrophone 457049 stops receiving detections. At this point, the particles began to spread out along hydrophone VR100's range. Since the particles spread evenly, their average does not move, so the error stays constant. Table 1 summarizes the distance errors and RMSE over the entire dataset and after the particles converged after approximately 61 seconds. After convergence, the RMSE dropped to approximately 10 meters.

5.2 Dynamic Dataset

Figures 6 and 7 follow the same format as figures 4 and 5, giving an overview of the dynamic dataset and plotting its estimation errors. As with the previous dataset, the top panel in Figure 6 shows the trajectories of the two hydrophones, the estimated and true trajectories of the tag, and the times at which detections occurred. The bottom panel in Figure 7 shows the times that GPS coordinates and detections where recorded. Unlike the static dataset, GPS coordinates were recorded continuously for the tag in this dataset. The dataset contains 39 detections from hydrophone 457049 and 23 detections from hydrophone VR100 spanning 349 seconds. Hydrophone 457049 received detections nearly continuously while hydrophone VR100 had some gaps in detections, the biggest of which occurred at about 100 seconds and lasted about a minute.

Figure 7 plots the errors for the dynamic dataset and highlights the state of the particle filter at 5 different times. Once again, the particles are initialized randomly at the start as seen in the panel at 0 seconds. After detections are received from both hydrophones, the particles converge around the overlap of the two ranges as seen in the second panel at 16 seconds. After some more time has passed and the tag and hydrophones have moved around relative to each other, most particles have converged around the true location. However, a small set of particles linger near the other point at which the two ranges overlap, as seen in the third panel at 41 seconds. As more detections are received, these particles are resampled away. When the gap in hydrophone VR100's detections occurs, hydrophone 457049 manages to continue accurately tracking the tag, as shown by the error plots in Figure 7 and by the positions of the particles in the last two lower panels. Table 2 summarizes the distance errors and RMSE over the entire dataset and after the particles converged after approximately 30 seconds.

The particle filter converges even when there are multiple clusters of particles at the two points where the hydrophone ranges overlap. It does so faster and more accurately when the tag itself is moving, as shown by the reduced RMSE after convergence in the dynamic dataset compared to the static dataset. As the hydrophones move, only a couple detections are necessary before most of the particles converge on the groundtruth location. Overall, the system has proven accurate, with state estimation and the integrated particle filter system having an accuracy of approximately 10m after convergence.

6 CONCLUSIONS

The ability to conduct fish tag localization off-line, after tracking experiments have been conducted, has been shown to be successful. However, the system has additional use as a state estimation system that can be run online and act as an input to the AUV's planning and control system. This would provide AUVs equipped with this newer, lower drag profile sensing system the ability to conduct real time autonomous tracking as done in our previous work. As in previous work, an AUV-to-AUV communication system will be needed.

While the system in place has a variety of potential applications, the possibility of extending it to marine-life tracking to better improve conservation efforts has proven extremely valuable. The compactness of the AUV and hydrophone combination opens new doors to speed and maneuvering capabilities and, by extension, a stealthier method of tracking which puts less stress on both the system and the surrounding environment. Further, these new capabilities allow for longer and more accurate missions. The accurate

and efficient system created herein will provide experts with a better understanding of wildlife behaviors and movement patterns. This knowledge will then assist with the identification of areas most suited for and requiring protection.

ACKNOWLEDGMENTS

This material is based on work supported by the National Science Foundation under Grant No. 1952616. Field experiments detailed in this work were performed at Alamitos Bay and Santa Elena Bay with assistance from CSU Long Beach Shark Lab and the University of Costa Rica. Preliminary tests of the system were conducted at the Robert J. Bernard Biological Field Station and Axelrood Aquatics Center at Roberts Pavilion.

REFERENCES

[1] Xiang Cao, Hongbing Sun, and G. Jan. 2018. Multi-AUV cooperative target search and tracking in unknown underwater environment. *Ocean Engineering* 150 (2018), 1–11.

[2] John H. Eiler, Thomas M. Grothues, Joseph A. Dobarro, and Rahul Shome. 2019. Tracking the Movements of Juvenile Chinook Salmon using an Autonomous Underwater Vehicle under Payload Control. *Applied Sciences* 9, 12 (2019). https://doi.org/10.3390/app9122516

[3] M. Espinoza, T. Farrugia, D. Webber, F. Smith, and C. Lowe. 2011. Testing a new acoustic telemetry technique to quantify long-term, fine-scale movements of aquatic animals. *Fisheries Research* 108 (2011), 364–371.

[4] O. Filatova, I. D. Fedutin, A. Burdin, and E. Hoyt. 2006. Using a mobile hydrophone stereo system for real-time acoustic localization of killer whales (Orcinus orca). *Applied Acoustics* 67 (2006), 1243–1248.

[5] Christina Forney, Esfandiar Manii, Michael Farris, M.A. Moline, Christopher G. Lowe, and Christopher M. Clark. 2012. Tracking of a tagged leopard shark with an AUV: Sensor calibration and state estimation. In *2012 IEEE International Conference on Robotics and Automation*. 5315–5321. https://doi.org/10.1109/ICRA.2012.6224991

[6] Thomas M. Grothues, Joseph Dobarro, John Ladd, Amanda Higgs, George Niezgoda, and Dan Miller. 2008. Use of a multi-sensored AUV to telemeter tagged Atlantic sturgeon and map their spawning habitat in the Hudson River, USA. In *2008 IEEE/OES Autonomous Underwater Vehicles*. 1–7. https://doi.org/10.1109/AUV.2008.5347597

[7] L. A. Hawkes, O. Exeter, S. M. Henderson, C. Kerry, A. Kukulya, J. Rudd, S. Whelan, N. Yoder, and M. J. Witt. 2020. Autonomous underwater videography and tracking of basking sharks. *Animal Biotelemetry* 8, 1 (17 Aug 2020), 29. https://doi.org/10.1186/s40317-020-00216-w

[8] K. Holland, C. Lowe, J. D. Peterson, and A. Gill. 1992. Tracking Coastal Sharks with small boats: Hammerhead Shark Pups as a case study. *Marine and Freshwater Research* 43 (1992), 61–66.

[9] Amy L. Kukulya, Roger Stokey, Carl Fiester, Edgar Mauricio Hoyos Padilla, and Gregory Skomal. 2016. Multi-vehicle autonomous tracking and filming of white sharks Carcharodon carcharias. In *2016 IEEE/OES Autonomous Underwater Vehicles (AUV)*. 423–430. https://doi.org/10.1109/AUV.2016.7778707

[10] Yukun Lin, Jerry Hsiung, Richard Piersall, Connor White, Christopher Lowe, and Christopher Clark. 2016. A Multi-Autonomous Underwater Vehicle System for Autonomous Tracking of Marine Life: A Multi-AUV System for Autonomous Tracking of Marine Life. *Journal of Field Robotics* 34 (08 2016). https://doi.org/10.1002/rob.21668

[11] Yukun Lin, H. Kastein, T. Peterson, C. Clark, H. Mudd, Connor F White, and C. Lowe. 2013. USING TIME OF FLIGHT DISTANCE CALCULATIONS FOR TAGGED SHARK LOCALIZATIONWITH AN AUV.

[12] Christopher G. Lowe and Richard N. Bray. 2006. *CHAPTER 20. Movement and Activity Patterns:*. University of California Press, 524–553. https://doi.org/doi:10.1525/9780520932470-022

[13] Emily N Meese and Christopher G Lowe. 2020. Active acoustic telemetry tracking and tri-axial accelerometers reveal fine-scale movement strategies of a non-obligate ram ventilator. *Movement Ecology* 8, 8 (feb 2020), 07KG05. https://doi.org/10.1186/s40462-020-0191-3

[14] J. Metcalfe and G. Arnold. 1997. Tracking fish with electronic tags. *Nature* 387 (1997), 665–666.

[15] B. Miller and S. Dawson. 2009. A large-aperture low-cost hydrophone array for tracking whales from small boats. *The Journal of the Acoustical Society of America* 126 5 (2009), 2248–56.

[16] Thomas P. Quinn and Richard D. Brodeur. 1991. Intra-specific Variations in the Movement Patterns of Marine Animals. (feb 1991), 231–241. https://doi.org/10.1093/icb/31.1.231

[17] Dylan Shinzaki, Chris Gage, Sarah Tang, Mark Moline, Barrett Wolfe, Christopher G. Lowe, and Christopher M. Clark. 2013. A multi-AUV system for cooperative tracking and following of leopard sharks. IEEE, 4153–4158. https://doi.org/10.1109/ICRA.2013.6631163

[18] Conner F White, Yukin Lin, Chris Clark, and Chris Lowe. 2015. Human vs robot: Comparing the viability and utility of autonomous underwater vehicles for the acoustic telemetry tracking of marine organisms. *Journal of Experimental Marine Biology and Ecology* (2015), 1–32. https://doi.org/10.1016/J.JEMBE.2016.08.010